A Semi-Degradable Composite Scaffold for Articular Cartilage Defects

Paul M. Scholten[1], **Kenneth W. Ng**[1], **Kiwon Joh**[1], **Lorenzo P. Serino**[2], **Russell F. Warren**[1], **Peter A. Torzilli**[1], and **Suzanne A. Maher**[1,†]

[1] Hospital for Special Surgery, New York, New York

[2] Department of Chemical Engineering, Industrial Chemistry and Materials Science, University of Pisa, Pisa, Italy

Abstract

Few options exist to replace or repair damaged articular cartilage. The optimal solution that has been suggested is a scaffold that can carry load and integrate with surrounding tissues; but such a construct has thus far been elusive. The objectives of this study were to manufacture and characterize a non-degradable hydrated scaffold. Our hypothesis was that the polymer content of the scaffold can be used to control its mechanical properties, while an internal porous network augmented with biological agents can facilitate integration with the host tissue. Using a two-step water-in-oil emulsion process a porous poly-vinyl alcohol (PVA) hydrogel scaffold combined with alginate microspheres was manufactured. The scaffold had a porosity of 11–30% with pore diameters of 107–187 μm, which readily allowed for movement of cells through the scaffold. Alginate microparticles were evenly distributed through the scaffold and allowed for the slow release of biological factors. The elastic modulus (E_s) and Poisson's ratio (υ), Aggregate modulus (H_a) and dynamic modulus (E_D) of the scaffold were significantly affected by % PVA, as it varied from 10% to 20% wt/vol. E_s and υ were similar to that of articular cartilage for both polymer concentrations, while H_a and E_D were similar to that of cartilage only at 20% PVA. The ability to control scaffold mechanical properties, while facilitating cellular migration suggest that this scaffold is a potentially viable candidate for the functional replacement of cartilage defects.

Introduction

Articular cartilage is a hydrated and lubricated tissue that allows for the relative movement of opposing joint surfaces under high loads [1–4]. Adult articular cartilage is avascular and lacks a source of mesenchymal cells[4–7], the consequences of which include impaired healing ability. Surgical techniques used to treat cartilage defects are aimed primarily at alleviating pain and have thus far not succeeded in preventing the progression to osteoarthritis[8–10]. Implantable scaffolds are being developed in an attempt to engineer replacement cartilage *ex vivo* by stimulating a cell-seeded scaffold prior to implantation[11–18] However, the ability of isolated chondrocytes to regenerate and organize extraceullar

†Corresponding author: Dr. Suzanne A. Maher, Hospital for Special Surgery, 535 E. 70th Street, New York, NY 10021, Tel: (212) 606-1083, Fax: (212) 249-2373, MaherS@hss.edu.

matrix components that mimic the complexity of native tissue either *in vivo* or *ex vivo* is unclear. Furthermore, the mechanical properties of the initial day 0 scaffolds developed so far have not yet matched that of the intact native tissue [19–21]. Thus, it is unknown if the scaffolds are able to carry joint loads at the time of implantation.

A non-degradable synthetic scaffold has been suggested as a potentially viable treatment to stabilize the site of a local defect[8]. The scaffold would ideally carry and distribute loads much in the way of the native tissue while providing a mechanism for long-term fixation. To this end, non-degradable hydrogel scaffolds (hydrophilic, crosslinked, hydrated, polymeric networks) have demonstrated promising *in vivo* animal model results[22],[23] although an inability to integrate with the surrounding tissue has been problematic[24]. A possible solution to this dilemma is to design a non-degradable hydrogel-based construct (to assist with load carrying ability) with an internal interconnected porous network (that can facilitate cell migration) and an ability to release biological agents (to encourage cell migration).

The objectives of this study were to manufacture and characterize a non-degradable hydrated scaffold combined with a degradable drug-delivery vehicle, a composite scaffold that we termed "semi-degradable." Our hypothesis was that the polymer content of the scaffold could be used to control its mechanical properties, while an internal porous network augmented with biological agents could facilitate integration with the host tissue.

Materials and Methods

Scaffold Manufacture

Manufacture of the scaffold required a two-phase process which included (i) formation of the alginate microparticles and (ii) construction of the PVA-alginate composite scaffold (Fig 1).

Alginate Microparticles—Alginate microspheres were formed using a standard water-in-oil emulsification technique. The oil phase – 110 ml of isooctane (Sigma Aldrich, St. Louis, MO) and 4 ml of Span 85 (Sigma Aldrich, St Louis, MO) – was added to a 250 ml round bottom flask which was submerged in an ice bath and stirred at 1000 rpm with an overhead mixer (RW20, IKA, Staufen, Germany). The water phase – 400 mg of alginic acid sodium salt from brown algae (Fluka, Sigma Aldrich, St. Louis, MO) in 14 ml of double distilled water and 6 ml of insulin (Humulin R 100 units/ml, Eli Lilly, Indianapolis, IN) – was added drop-wise to the oil phase and the combined solution was stirred for 10 minutes. A surfactant – 12 ml of Tween 85 (Sigma Aldrich, St Louis, MO) – and a crosslinking agent – 2 g of calcium chloride (Sigma Aldrich, St Louis, MO) in 20 ml of double distilled water – were added drop-wise and the solution was stirred for 25 minutes and allowed to rest for 45 minutes. The upper liquid (organic phase) was decanted from the flask and discarded. The remaining solution was twice mixed with isooctane and once with ethanol, centrifuged and the supernatant was discarded. The pellet was allowed to air dry at room temperature under a chemical hood and the resulting microspheres were stored at 4°C.

PVA-Alginate scaffold—To create the PVA solutions, 3 g (for a 10% wt/vol solution) or 6 g (for a 20% solution) of PVA powder (Elvanol 71–30; DuPont, Wilmington, DE;

Mw~96000) was dissolved into 30 ml of deionized water. The solutions were autoclaved for 1 hour at 120°C and allowed to cool at room temperature. Alginate microspheres (100 wt% of PVA) were added to the PVA solutions and mixed for 5 min at 500 rpm. The solutions were allowed to settle for 1 minute, the overhead mixer was set to 150 rpm, and 6 ml of dichloromethane (DCM; Sigma Aldrich, St Louis, MO) was added drop-wise as the mixture was stirred for 3 minutes. For the 20% PVA scaffolds, a separate mixing station was used with the mixing speed increased to 300 rpm due to the higher viscosity of the polymer solution. The final emulsions were poured into individual wells of a 24-well polystyrene plate and subjected to 5 freeze/thaw cycles (MicroClimate chamber, Cincinnati Sub-Zero, Cincinnati, OH), consisting of 23 hours at −25°C followed by one hour at 25°C. Twenty-four samples of each gel concentration were manufactured in 6 batches using this technique: four were used for morphological analysis, six were used for mechanical evaluation, six for assessment of growth factor release rate, and eight to assess the cellular response.

Morphology

The top and bottom surfaces of the scaffolds were removed with a scalpel to create a 5 mm thick disc for morphological analysis (one from each of 4 different batches of material). The scaffold discs were imaged in the environmental chamber of a scanning electron microscope (FEI Philips, Hillsboro, OR). The pore diameter and microparticle size distribution were measured with ImageJ (National Institute of Health, Bethesda, MD), and percent porosity was determined by calculating the total area of the pores to the area of the field of view.

Mechanical Testing

Scaffolds (n = 6) were cored using a 5-mm diameter biopsy punch and sliced to a thickness of 2–3 mm on a freezing stage sledge microtome to ensure flat parallel surfaces. Full thickness disks of articular cartilage (n=6) were harvested from the trochlea of mature bovine knees using a 5 mm biopsy punch. Tissue was removed from the top and bottom surfaces of the scaffold using a freezing stage microtome to ensure flat, parallel surfaces. This resulted in tissue thicknesses of 1–2 mm. All samples were subjected to a series of stress relaxation tests under confined and unconfined conditions using a custom-built test apparatus, the Compression Computer Automated Soft Tissue Test System[25].

For unconfined compression testing, samples were placed on a stainless steel base and loaded with a polished stainless steel platen (d = 10-mm). The surface of each sample was detected using a trigger-load of 1.5 g and this position was used to determine the construct initial thickness (h_0) and defined as the zero-strain, zero-stress state. Then, a tare strain of 8% h_0 was applied in two 4% ramps and held until the load reached a steady-value, defined throughout testing as a change in average force of less than 0.5 g for 180 s. Each sample was then subjected to 3 sequential step compressions of 4% h_0 at a velocity of 20 μm s^{-1}. For each step, time-displacement-load data was collected at a frequency of 20 Hz for the first 5 seconds and at 0.2 Hz thereafter until equilibrium was reached. Samples were kept immersed in phosphate buffered saline (PBS) throughout testing. After completion of the unconfined test the sample was allowed to return to its original thickness. The confined compression test used a confining stainless-steel chamber and a porous 5 mm diameter brass filter and followed the same testing protocol used for the unconfined test.

The equilibrium stress for each step was plotted as a function of the equilibrium strain. Elastic modulus (E_s) and Aggregate modulus (H_a) were determined for each sample from the slope of the best fit line from the equilibrium stress-strain response for the three compression steps for unconfined and confined conditions, respectively. Poisson's ratio (ν_s) was calculated using the following formula [26]: ⬛⬛⬛⬛⬛. Displacement-load data for the confined condition was further analyzed using the biphasic theory[27] to determine the permeability at each step. In addition, the slope of the stress-strain curve during the ramping phase for each compression step for both unconfined and confined testing was calculated and defined as the dynamic modulus (E_D).

Release of growth factors

The scaffolds (n=6) were sliced on a freezing stage microtome to a thickness of 8.5 mm and cored to a diameter of 10 mm. The samples were placed in 5 mL of phosphate buffered saline solution and incubated at 37°C. The entire solution was mildly vortexed, collected, stored and replaced with another 5 mL of PBS at the following time-points: every hour for the first seven hours, every 24 hours for the first 14 days, and once a week for the first four weeks. Using a Coomassie Plus protein assay (Pierce, Rockford, IL), the amount of insulin in the collected solution was quantified as a function of time. Non-linear regression was used to model the time dependent release of growth factors (SigmaPlot, Systat Software, Inc., San Jose, CA).

Cell Response

Scaffolds (n=8) containing alginate microparticles without insulin were sliced and pre-soaked in DMEM/F12 media containing 10% antibiotics/antimycotic and washed at 4°C for 24 hours. Ten million ATDC5 cells (a murine chondrogenic cell line[28]) were injected at three evenly spaced locations along the side of the scaffolds with a 18 gauge syringe, placed in media containing 10% fetal bovine serum and 1% antibiotics/antimycotic, and incubated at 37°C. The samples were collected after 14 days, washed, fixed overnight with 4% paraformaldehyde containing cacodylate buffer, washed in double distilled water, paraffin embedded, sliced (longitudinally & transversely) to a thickness of 7 μm, and stained using hematoxylin and eosin.

Analysis of Data

A Mann-Whitney Rank Sum Test was used to assess differences in Elastic modulus, Aggregate modulus, Dynamic modulus, and Poisson's ratio between scaffolds and mature bovine cartilage. A Wilcoxon test was used to assess paired differences in the theoretical (from the biphasic theory) and experimental Aggregate modulus and dynamic modulus of scaffolds and bovine cartilage. A Spearman rank order correlation coefficient test was performed to determine if a relationship exists between permeability and compressive strain. Parameters are reported as mean ± standard deviation.

Results

Morphology

The method of manufacture resulted in a porous scaffold with an even distribution of microparticles throughout both gel concentrations (Fig. 2, only 10% PVA shown). Average pore diameter was 147 ± 40 μm and the percent porosity determined from these macropores under ESEM ranged from 11% to 30% with no significant differences in these parameters between gel concentration; alginate microspheres had an average diameter of 15 ± 4 μm. Water content of the gels was ~90% for both 10% PVA and 20 % PVA hydrogels.

Mechanical Testing

The biphasic theory provided an excellent fit to the stress-relaxation data (Fig. 3). There was a linear relationship between stress and strain at equilibrium for unconfined and confined conditions; from which E_s and H_a were calculated. H_a was significantly higher for bovine articular cartilage (0.21 ± 0.07 MPa) and 20% PVA constructs (0.16 ± 0.02 MPa) compared to that of the 10% PVA scaffolds (0.06 ± 0.01 MPa; $p=0.002$), but there was no statistically significant difference between articular cartilage and the 20% PVA scaffolds (Fig. 4). For E_s, the 20% PVA scaffold was significantly stiffer than the 10% PVA scaffold (0.14 ± 0.02 vs. 0.04 ± 0.01 MPa, $p<0.05$), and there was no significant difference between either scaffold type and articular cartilage (0.11 ± 0.06 MPa, $p>0.10$, Fig. 4). E_D was significantly higher for articular cartilage when compared to that of the scaffolds at each step under unconfined testing (Table 1). Under confined compression conditions, however, the 20% PVA scaffolds were found to have no statistical differences in modulus values compared to articular cartilage at all tested strain levels ($p>0.20$).

Scaffold permeability for the 10% PVA hydrogels was $0.099 \pm 0.116 \times 10^{-14}$ m^4/N-sec and was not affected by % strain ($p > 0.05$). As expected, the permeability of bovine cartilage decreased as compressive strain increased with average values ranging from 0.20 to 0.005×10^{-14} m^{4}N/s (Table 2). This strain-dependent behavior was also observed for the 20% PVA scaffolds as well (Table 2). There was no statistical difference between the theoretical and experimental aggregate modulus and dynamic modulus values (not shown), indicating a good fit between the behavior of the biphasic theory and experimental data for all scaffolds and cartilage samples. There was no statistically significant difference between the Poisson's ratio of the scaffolds (10% PVA: 0.29 ± 0.10, 20% PVA: 0.22 ± 0.07) and articular cartilage (0.37 ± 0.09, $p>0.15$).

Release of Growth Factors

Insulin release was detected within the first hour of incubation. Nonlinear regression of the time dependent release of insulin produced equation (1):

(1)

where $b=0.0277$/hour ± 0.0086. At 25 hours, 50% of the total encapsulated insulin had been released (Fig. 5).

Cell Response

Histological analysis of the cell seeded scaffolds revealed viable cells within and on top of the scaffold. Cells appeared to have started to migrate from their points of injection through the scaffold's open pores by 14 days after seeding (Fig. 6).

Discussion

The objective of our study was to design a porous, hydrated, non-degradable composite scaffold that could mechanically function to carry joint loads and encourage host-tissue integration when implanted into an articular cartilage defect. A non-degradable porous poly-vinyl alcohol (PVA) hydrogel combined with degradable alginate microparticles was designed and its mechanical properties, ability to release biological agents, and cellular response were assessed. The elastic modulus (E_s) and Poisson's ratio of the scaffold were similar to that of articular cartilage for both hydrogel concentrations used in the study, while the Aggregate modulus (H_a) was comparable to that of cartilage for the 20% PVA concentration. Increasing the concentration of the PVA resulted in the scaffold possessing a similar dynamic modulus (E_D) under confined compression to that of cartilage at all of the strains tested. The morphology of the scaffold was reproducible, with pores ranging in size from 107 – 187 μm, microparticles from 11 – 19 μm, and a percent porosity of the macropores from 11% to 30%. These morphological characteristics lent themselves readily to the movement of cells through the scaffold, which occurred after 14 days. Finally, biological factors incorporated into the alginate microparticles were released in a controlled and reproducible manner, which will likely help encourage cell migration in a controlled manner. These suggest that this scaffold is a potentially viable candidate for the functional replacement of cartilage defects given the ability to control both mechanical properties and overall scaffold morphology.

Poly(vinyl alcohol), PVA, was chosen for the manufacture of the scaffold because it is a biocompatible, stable, nontoxic material that is currently used in several biomedical applications, including contact lenses[29], wound healing[30], tendon repair[31],[32], as a soluble stent in microvascular anastomoses[33], and in a number of central nervous system applications[34]. Non-porous PVA-based hydrogels have also been previously explored for the treatment of cartilage defects. Noguchi et al.[23], and Oka et al.[35], found that PVA scaffolds inserted into an osteochondral defect in rabbits and dogs remained intact after 24 and 52 weeks of implantation, respectively. However, the response of the underlying bone to the scaffold (an indicator of fixation), and the histological appearance of the cartilage adjacent to the scaffold (an indicator of wear performance) were not described. More recently, we reported the formation of a fibrous membrane surrounding the walls of non-porous PVA scaffolds placed into osteochondral defects in rabbits [24]. To avoid the formation of a membrane and to encourage robust integration with surrounding musculoskeletal tissues we developed a porous version of that scaffold [36]. However, the challenge of matrix integration across the scaffold-cartilage interface is not trivial. Methods such as enzymatically digesting cartilage to help free cells from their dense matrix [37],[38], encouraging cell migration in response to a growth factor gradient [39], and the adhesives have been explored in the literature.

In designing the third generation scaffold as presented in this study, we chose to integrate alginate microparticles for growth factor release along with a porous structure that would facilitate inward cellular migration. We have demonstrated the ability to reproducibly manufacture a scaffold with an average macropore porosity of 17% and an average pore diameter of 147 μm – which is sufficiently large to allow for the migration of chondrocytes (10 to 30 μm in diameter [40]). In addition, the overall construct permeability was found to be in the range of native articular cartilage. The pore size measured in this study was also within the range found by Lee et al., who observed chondrocyte proliferation within scaffolds containing pore sizes ranging from 50 to 250 μm [13]. Optimal pore size for chondrocyte migration remains unknown, but Lien et al. have shown that the rate of cell growth and amount of GAG secretion increases with increasing pore size in gelatin scaffolds with a maximal response observed in scaffolds having the largest pore size tested (250 to 500 μm)[41]. Others have suggested that smaller pores may be better to optimize cell-to-cell interactions and chondrogenesis [42]. Analysis of the cellular response demonstrated cell viability within the construct up to 14 days after initial seeding. Cells appeared to migrate into the scaffold from the injection ports and then proliferate within the scaffold forming cell clusters, further suggesting that the morphology supports cellular viability and migration. Cell attachment onto PVA has been shown to be increased with the incorporation of fibronectin and other types of cell-surface attachment ligands [43]–[45]. The addition of cell-ligands is planned for future experiments.

Alginates are water-soluble polysaccharides that can form gels by reaction with divalent cations such as Ca^{2+}, Sr^{2+}, or Ba^{2+} [46]. Alginate microparticles were chosen for this study because they have been extensively investigated as a hydrophilic-drug delivery system owing to their non-toxicity, biocompatibility and biodegradability[47],[48] and their ability to retain the biological activity of biological agents. The inclusion of insulin loaded alginate microspheres in our PVA scaffolds facilitated continued insulin release over a 3 week period, with 90% of the insulin released within the first 7 days, and a steady-state release thereafter. This release profile is similar to that measured in other studies [49], and could be used to enhance the ability of cells to migrate through and to synthesize matrix within the scaffold when the microparticles are loaded with the appropriate growth factor or chemo-tactic/attractant factors. This will be explored in future experiments.

Aside from achieving integration with host tissue, any scaffold for placement into a cartilage defect should ideally carry loads much in the way of the native tissue. Though other researchers have measured the mechanical characteristics of PVA hydrogels [50]–[54], the differences in scaffold manufacture and mechanical tests (e.g., shear, tensile, compressive) have limited our ability to directly compare the gel properties with our colleagues in this area. Therefore, we evaluated the mechanical properties of the scaffold and compared them to that of articular cartilage as a reference. Since undamaged human articular cartilage samples are difficult to obtain, for the purposes of this study, the scaffold's mechanical response was compared to that of mature bovine articular cartilage. Samples were tested in unconfined and confined compression configurations and subjected to a series of stress relaxation tests at three strains. The mechanical properties both under equilibrium and dynamic loading conditions were found to increase with increasing gel concentration with the 20% PVA having moduli values comparable to the bovine cartilage tested in this study.

This is promising in that modifying the gel concentration (tuning) may allow for a wide range of stiffness values. In particular, the 20% PVA in confined compression, which approximates filling a cartilage defect, had a measured dynamic modulus that compares favorably to values obtained for bovine cartilage in our experiments.

There were limitations in our study. The processes used to manufacture the scaffold, involves the used of dichloromethane (DCM), which is a toxic organic solvent. The scaffold must be washed in media for at least 24 hours prior to use and, though no negative cellular response was noted, this washing would allow for the loss of some of the included growth factor. Other authors have demonstrated that techniques such as the addition of polyethylene glycol [55] or salt/particle leaching methods [56] can create porous networks within the PVA hydrogels and similar approaches will be explored by our laboratory in the future. Furthermore, the mechanical properties of the scaffold were compared to that of bovine cartilage. Given that the mechanical properties of articular cartilage are highly dependent on the source of tissue, its extracellular matrix content [57], and the conditions under which it is tested [58,59], comparison with human cartilage would be ideal. In regards to the dynamic moduli values measured in our study, we used the slope of the stress-strain curve during the ramping phase of compression to calculate the unconfined and confined dynamic moduli. Other testing methods to determine this structural property for both cartilage and tissue engineered scaffolds have involved subjecting the material to oscillatory compression[59–61] which may provide a better estimate of the *in vivo* dynamic modulus. Also, no mechanical tests were performed to determine the tensile properties of our scaffold. Our cell-based studies were designed to ensure that scaffold morphology was sufficient to support cell migration; as such we did not assess the response of cells to the release of the insulin from within the alginate microparticles. It may be possible that there was an effect of the insulin on cell motility similar to that reported for insulin-like growth factor I [62,63]. Finally, further analysis is needed to study the degree of interconnectivity of the pores, such as via mercury porousimetry or other techniques.

In conclusion, we have demonstrated the ability to reproducibly manufacture a porous, hydrated composite scaffold as a replacement for articular cartilage defects. The scaffold contained pores sufficient for cellular migration, had mechanical properties that within the realm of that of articular cartilage, and could support the long-term release of bioactive agents. This scaffold is a suggested as a viable candidate for the functional replacement of cartilage defects.

Acknowledgments

References

1. Mow VC, Ateshian GA, Spilker RL. Biomechanics of diarthrodial joints: a review of twenty years of progress. Journal of Biomechanical Engineering. 1993; 115(4B):460. [PubMed: 8302026]

2. Gilley JS, Gelman MI, Edson DM, Metcalf RW. Chondral fractures of the knee. Arthrographic, arthroscopic, and clinical manifestations. Radiology. 1981; 138(1):51. [PubMed: 7455096]

3. Shelbourne KD, Jari S, Gray T. Outcome of untreated traumatic articular cartilage defects of the knee: a natural history study. The Journal of bone and joint surgery. American volume. 2003; 85-A(Suppl 2):8. [PubMed: 12721340]

4. Buckwalter JA, Mankin HJ. Articular cartilage: tissue design and chondrocyte-matrix interactions. Instructional course lectures. 1998; 47:477. [PubMed: 9571449]

5. Mankin, HJ.; Mow, VC.; Buckwalter, JA.; Iannotti, JP.; Ratcliffe, A. Form and Function of Articular Cartilage. In: Simon, SR., editor. Orthopaedic Basic Science. Rosemont, Ill: American Academy of Orthopaedic Surgeons; 1994. p. 1-44.

6. Mankin HJ. The response of articular cartilage to mechanical injury. The Journal of bone and joint surgery American volume. 1982; 64(3):460. [PubMed: 6174527]

7. Buckwalter, JA.; Rosenberg, LC.; Hunziker, EB. Articular cartilage: composition, structure, response to injury, and methods to facilitating repair. In: Ewing, JW., editor. Articular cartilage and knee joint function : basic science and arthroscopy. New York: Raven Press; 1990. p. 19-56.

8. Wright TM, Maher SA. Current and novel approaches to treating chondral lesions. J Bone Joint Surg Am. 2009; 91 (Suppl 1):120–5. [PubMed: 19182038]

9. Mow, VC.; Proctor, CS.; Kelly, MA. Biomechanics of Articular Cartilage. In: Nordin, M.; Frankel, VH., editors. Biomechanics of articular cartilage. Philadelphia: Lea and Febige; 1989. p. 31-58.

10. Miller, RH., III; Azar, FM. Sports Medicine: Knee Injuries: Articular Cartilage Injuries. In: Campbell, WC.; Canale, ST.; Beaty, JH., editors. Campbell's Operative Orthopaedics. Philadelphia, PA: Mosby/Elsevier; 2008. p. 2553

11. Kang Y, Yang J, Khan S, Anissian L, Ameer GA. A new biodegradable polyester elastomer for cartilage tissue engineering. J Biomed Mater Res A. 2006; 77(2):331–9. [PubMed: 16404714]

12. Lebourg M, Sabater Serra R, Mas Estelles J, Hernandez Sanchez F, Gomez Ribelles JL, Suay Anton J. Biodegradable polycaprolactone scaffold with controlled porosity obtained by modified particle-leaching technique. J Mater Sci Mater Med. 2008; 19(5):2047–53. [PubMed: 17968506]

13. Lee CT, Huang CP, Lee YD. Biomimetic porous scaffolds made from poly(L-lactide)-g-chondroitin sulfate blend with poly(L-lactide) for cartilage tissue engineering. Biomacromolecules. 2006; 7(7):2200–9. [PubMed: 16827588]

14. Xie J, Ihara M, Jung Y, Kwon IK, Kim SH, Kim YH, Matsuda T. Mechano-active scaffold design based on microporous poly(L-lactide-co-epsilon-caprolactone) for articular cartilage tissue engineering: dependence of porosity on compression force-applied mechanical behaviors. Tissue Eng. 2006; 12(3):449–58. [PubMed: 16579678]

15. Angele P, Kujat R, Nerlich M, Yoo J, Goldberg V, Johnstone B. Engineering of osteochondral tissue with bone marrow mesenchymal progenitor cells in a derivatized hyaluronan-gelatin composite sponge. Tissue Eng. 1999; 5(6):545–54. [PubMed: 10611546]

16. Grande DA, Halberstadt C, Naughton G, Schwartz R, Manji R. Evaluation of matrix scaffolds for tissue engineering of articular cartilage grafts. J Biomed Mater Res. 1997; 34(2):211–20. [PubMed: 9029301]

17. Rotter N, Aigner J, Naumann A, Planck H, Hammer C, Burmester G, Sittinger M. Cartilage reconstruction in head and neck surgery: comparison of resorbable polymer scaffolds for tissue engineering of human septal cartilage. J Biomed Mater Res. 1998; 42(3):347–56. [PubMed: 9788496]

18. Sittinger M, Reitzel D, Dauner M, Hierlemann H, Hammer C, Kastenbauer E, Planck H, Burmester GR, Bujia J. Resorbable polyesters in cartilage engineering: affinity and biocompatibility of polymer fiber structures to chondrocytes. J Biomed Mater Res. 1996; 33(2):57–63. [PubMed: 8736023]

19. LeRoux MA, Guilak F, Setton LA. Compressive and shear properties of alginate gel: effects of sodium ions and alginate concentration. J Biomed Mater Res. 1999; 47(1):46–53. [PubMed: 10400879]

20. Pei M, Solchaga LA, Seidel J, Zeng L, Vunjak-Novakovic G, Caplan AI, Freed LE. Bioreactors mediate the effectiveness of tissue engineering scaffolds. FASEB J. 2002; 16(12):1691–4. [PubMed: 12207008]

21. Mauck RL, Soltz MA, Wang CC, Wong DD, Chao PH, Valhmu WB, Hung CT, Ateshian GA. Functional tissue engineering of articular cartilage through dynamic loading of chondrocyte-seeded agarose gels. J Biomech Eng. 2000; 122(3):252–60. [PubMed: 10923293]

22. Oka M, Noguchi T, Kumar P, Ikeuchi K, Yamamuro T, Hyon SH, Ikada Y. Development of an artificial articular cartilage. Clin Mater. 1990; 6(4):361–81. [PubMed: 10171540]

23. Noguchi T, Yamamuro T, Oka M, Kumar P, Kotoura Y, Hyon S, Ikada Y. Poly(vinyl alcohol) hydrogel as an artificial articular cartilage: evaluation of biocompatibility. J Appl Biomater. 1991; 2(2):101–7. [PubMed: 10171121]

24. Maher SA, Doty SB, Torzilli PA, Thornton S, Lowman AM, Thomas JD, Warren R, Wright TM, Myers E. Nondegradable hydrogels for the treatment of focal cartilage defects. Journal of biomedical materials research Part A. 2007; 83(1):145. [PubMed: 17390320]

25. Torzilli, PA. Measurement of the compressive properties of thin cartilage slices: evaluating tissue inhomogeneity. In: Maroudas, AK., editor. Cartilage Methods. New York: Academic Press; 1990. p. 304-308.

26. Jurvelin JS, Buschmann MD, Hunziker EB. Optical and mechanical determination of Poisson's ratio of adult bovine humeral articular cartilage. Journal of Biomechanics. 1997; 30(3):235. [PubMed: 9119822]

27. Mow, VC. Journal of Biomechanical Engineering. Vol. 102. New York, N. Y: American Society of Mechanical Engineers; 1980. Biphasic creep and stress relaxation of articular cartilage in compression? Theory and experiments; p. 73

28. Atsumi T, Miwa Y, Kimata K, Ikawa Y. A chondrogenic cell line derived from a differentiating culture of AT805 teratocarcinoma cells. Cell Differ Dev. 1990; 30(2):109–16. [PubMed: 2201423]

29. Hyon SH, Cha WI, Ikada Y, Kita M, Ogura Y, Honda Y. Poly(vinyl alcohol) hydrogels as soft contact lens material. J Biomater Sci Polym Ed. 1994; 5(5):397–406. [PubMed: 8038135]

30. Bourke SL, Al-Khalili M, Briggs T, Michniak BB, Kohn J, Poole-Warren LA. A photo-crosslinked poly(vinyl alcohol) hydrogel growth factor release vehicle for wound healing applications. AAPS PharmSci. 2003; 5(4):E33. [PubMed: 15198521]

31. Kobayashi M, Toguchida J, Oka M. Development of polyvinyl alcohol-hydrogel (PVA-H) shields with a high water content for tendon injury repair. J Hand Surg [Br]. 2001; 26(5):436–40.

32. Kobayashi M, Toguchida J, Oka M. Development of the shields for tendon injury repair using polyvinyl alcohol--hydrogel (PVA-H). J Biomed Mater Res. 2001; 58(4):344–51. [PubMed: 11410891]

33. Yamagata S, Handa H, Taki W, Yonekawa Y, Ikada Y, Iwata H. Experimental nonsuture microvascular anastomosis using a soluble PVA tube and plastic adhesive. J Microsurg. 1979; 1(3):208–15. [PubMed: 16317947]

34. Nunamaker E, Purcell E, Kipke D. In vivo stability and biocompatibility of implanted calcium alginate disks. J Biomed Mater Res A. 2007; 83(4):1128–37. [PubMed: 17595019]

35. Oka M, Chang YS, Nakamura T, Ushio K, Toguchida J, Gu HO. Synthetic osteochondral replacement of the femoral articular surface. J Bone Joint Surg Br. 1997; 79(6):1003–7. [PubMed: 9393921]

36. Charlton DC, Peterson MG, Spiller K, Lowman A, Torzilli PA, Maher SA. Semi-Degradable Scaffold for Articular Cartilage Replacement. Tissue engineering. 2007

37. Bos PK, DeGroot J, Budde M, Verhaar JA, van Osch GJ. Specific enzymatic treatment of bovine and human articular cartilage: implications for integrative cartilage repair. Arthritis Rheum. 2002; 46(4):976–85. [PubMed: 11953975]

38. van de Breevaart Bravenboer J, In der Maur CD, Bos PK, van Resen IH, Weinans H, Feenstra L, Verhaar JA, van Osch GJ. Increased Interfacial Strength Of Transplanted Cartilage. Vivo Following Enzymatic Treatment Of Wound Edges. 2003:0188.

39. Holland TA, Tabata Y, Mikos AG. Dual growth factor delivery from degradable oligo(poly(ethylene glycol) fumarate) hydrogel scaffolds for cartilage tissue engineering. J Control Release. 2005; 101(1–3):111–25. [PubMed: 15588898]

40. Stockwell, RA. Biology of cartilage cells. Vol. viii. Cambridge; New York: Cambridge University Press; 1979. p. 329

41. Lien S, Ko L, Huang T. Effect of pore size on ECM secretion and cell growth in gelatin scaffold for articular cartilage tissue engineering. Acta Biomater. 2008

42. Vickers S, Squitieri L, Spector M. Effects of cross-linking type II collagen-GAG scaffolds on chondrogenesis in vitro: dynamic pore reduction promotes cartilage formation. Tissue Eng. 2006; 12(5):1345–55. [PubMed: 16771647]

43. Charlton D, Kim M, Attia E, Torzilli PA, Peterson M, Pleshko Camacho N, Maher SA. Incorporation of FN into PVA scaffolds enhances chondrocyte adhesion. Trans Orthop Res. 2007; 32:1569.

44. Nuttelman CR, Henry SM, Anseth KS. Synthesis and characterization of photocrosslinkable, degradable poly(vinyl alcohol)-based tissue engineering scaffolds. Biomaterials. 2002; 23(17): 3617–26. [PubMed: 12109687]

45. Schmedlen RH, Masters KS, West JL. Photocrosslinkable polyvinyl alcohol hydrogels that can be modified with cell adhesion peptides for use in tissue engineering. Biomaterials. 2002; 23(22): 4325–32. [PubMed: 12219822]

46. Smidsrød O. Molecular basis for some physical properties of alginates in the gel state. Faraday discussions of the Chemical Society. 1974; 57:263–274.

47. Chitkara D, Shikanov A, Kumar N, Domb AJ. Biodegradable injectable in situ depot-forming drug delivery systems. Macromol Biosci. 2006; 6(12):977–90. [PubMed: 17128422]

48. George M, Abraham TE. Polyionic hydrocolloids for the intestinal delivery of protein drugs: alginate and chitosan--a review. J Control Release. 2006; 114(1):1–14. [PubMed: 16828914]

49. Rasmussen MR, Snabe T, Pedersen LH. Numerical modelling of insulin and amyloglucosidase release from swelling Ca-alginate beads. J Control Release. 2003; 91(3):395–405. [PubMed: 12932717]

50. Bodugoz-Senturk H, Macias CE, Kung JH, Muratoglu OK. Poly(vinyl alcohol)-acrylamide hydrogels as load-bearing cartilage substitute. Biomaterials. 2009; 30(4):589–96. [PubMed: 18996584]

51. Joshi A, Fussell G, Thomas J, Hsuan A, Lowman A, Karduna A, Vresilovic E, Marcolongo M. Functional compressive mechanics of a PVA/PVP nucleus pulposus replacement. Biomaterials. 2006; 27(2):176. [PubMed: 16115678]

52. Lee SY, Pereira BP, Yusof N, Selvaratnam L, Yu Z, Abbas AA, Kamarul T. Unconfined compression properties of a porous poly(vinyl alcohol)-chitosan-based hydrogel after hydration. Acta Biomater. 2009; 5(6):1919–25. [PubMed: 19289306]

53. Stammen JA, Williams S, Ku DN, Guldberg RE. Mechanical properties of a novel PVA hydrogel in shear and unconfined compression. Biomaterials. 2001; 22(8):799. [PubMed: 11246948]

54. Millon LE, Oates CJ, Wan W. Compression properties of polyvinyl alcohol--bacterial cellulose nanocomposite. J Biomed Mater Res B Appl Biomater. 2009; 90(2):922–9. [PubMed: 19360889]

55. Bodugoz-Senturk H, Choi J, Oral E, Kung JH, Macias CE, Braithwaite G, Muratoglu OK. The effect of polyethylene glycol on the stability of pores in polyvinyl alcohol hydrogels during annealing. Biomaterials. 2008; 29(2):141–9. [PubMed: 17950839]

56. Oh SH, Kang SG, Kim ES, Cho SH, Lee JH. Fabrication and characterization of hydrophilic poly(lactic-co-glycolic acid)/poly(vinyl alcohol) blend cell scaffolds by melt-molding particulate-leaching method. Biomaterials. 2003; 24(22):4011–21. [PubMed: 12834596]

57. Appleyard RC, Burkhardt D, Ghosh P, Read R, Cake M, Swain MV, Murrell GA. Topographical analysis of the structural, biochemical and dynamic biomechanical properties of cartilage in an ovine model of osteoarthritis. Osteoarthritis Cartilage. 2003; 11(1):65–77. [PubMed: 12505489]

58. Korhonen R, Laasanen M, Töyräs J, Rieppo J, Hirvonen J, Helminen H, Jurvelin J. Comparison of the equilibrium response of articular cartilage in unconfined compression, confined compression and indentation. J Biomech. 2002; 35(7):903–9. [PubMed: 12052392]

59. Park S, Hung CT, Ateshian GA. Mechanical response of bovine articular cartilage under dynamic unconfined compression loading at physiological stress levels. Osteoarthritis Cartilage. 2004; 12(1):65–73. [PubMed: 14697684]

60. Mauck RL, Wang CC, Oswald ES, Ateshian GA, Hung CT. The role of cell seeding density and nutrient supply for articular cartilage tissue engineering with deformational loading. Osteoarthritis Cartilage. 2003; 11(12):879–90. [PubMed: 14629964]

61. Ng KW, Kugler LE, Doty SB, Ateshian GA, Hung CT. Scaffold degradation elevates the collagen content and dynamic compressive modulus in engineered articular cartilage. Osteoarthritis Cartilage. 2009; 17(2):220–7. [PubMed: 18801665]

62. Chang C, Lauffenburger DA, Morales TI. Motile chondrocytes from newborn calf: migration properties and synthesis of collagen II. Osteoarthritis Cartilage. 2003; 11(8):603–12. [PubMed: 12880583]

63. Mishima Y, Lotz M. Chemotaxis of human articular chondrocytes and mesenchymal stem cells. J Orthop Res. 2008; 26(10):1407–12. [PubMed: 18464249]
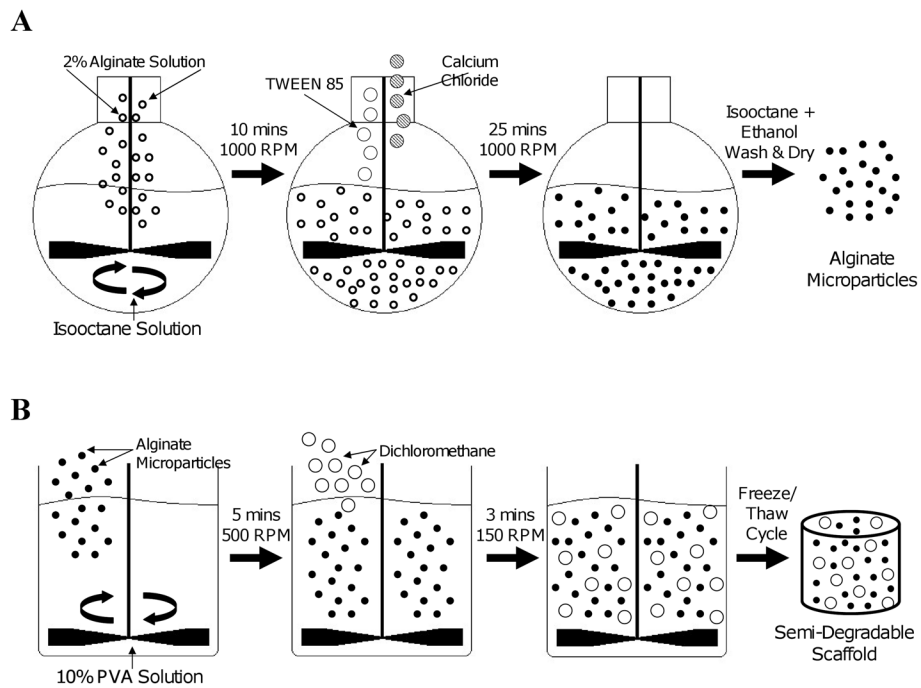
A

B

Figure 1.
Method of scaffold manufacture. A water-in-oil emulsion technique (A) was used to create the alginate microparticles. These drug-delivery particles were then added during PVA hydrogel fabrication (B) to create the final semi-degradable scaffold.
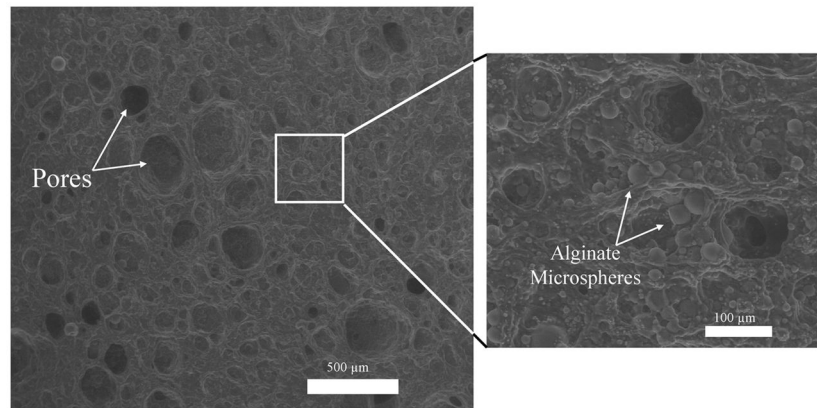
Figure 2.
Using ESEM, macropores and embedded alginate microparticles were evident in the hydrated PVA scaffolds. The scaffolds had an average pore size of 147 ± 40 μm; percent porosity of these macropores ranged from 11% to 30%. Alginate microspheres had an average diameter of 15 ± 4 μm.
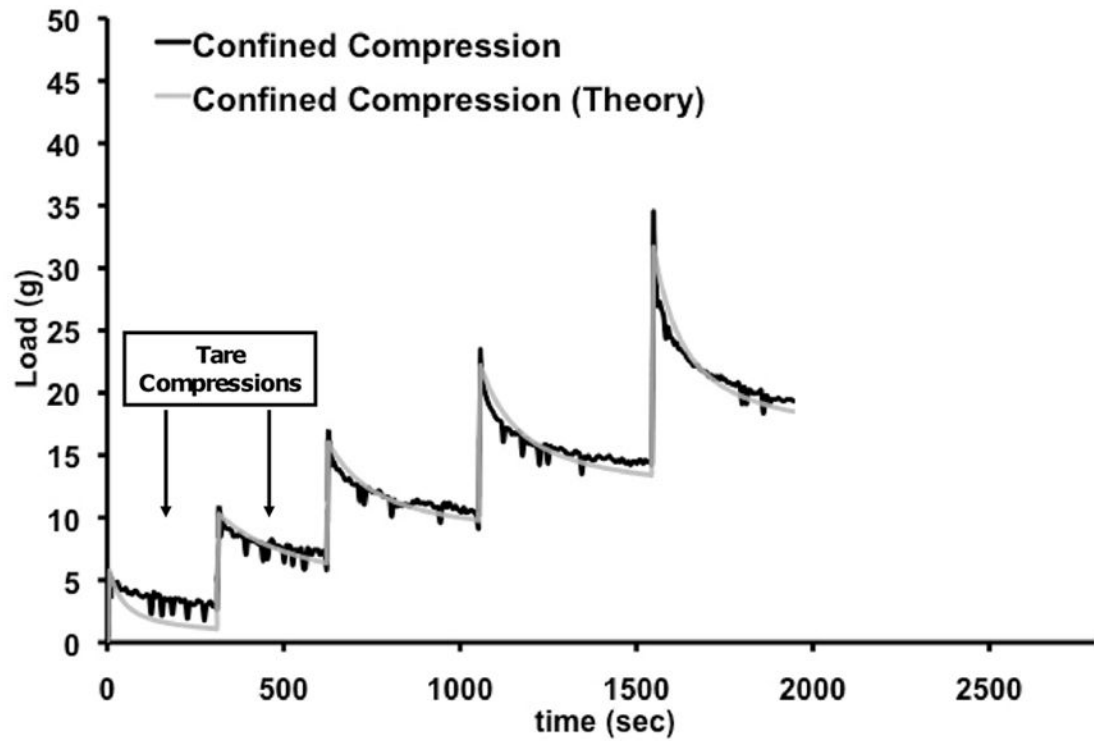
Figure 3.
Response of scaffold to stress-relaxation tests in confined and unconfined configuration of a representative construct. The experimental data and theoretical fit as per the biphasic theory for the confined tests are illustrated. The first two ramps represent the 8% tare strain (applied in two 4% strain steps) and were not used for calculations.
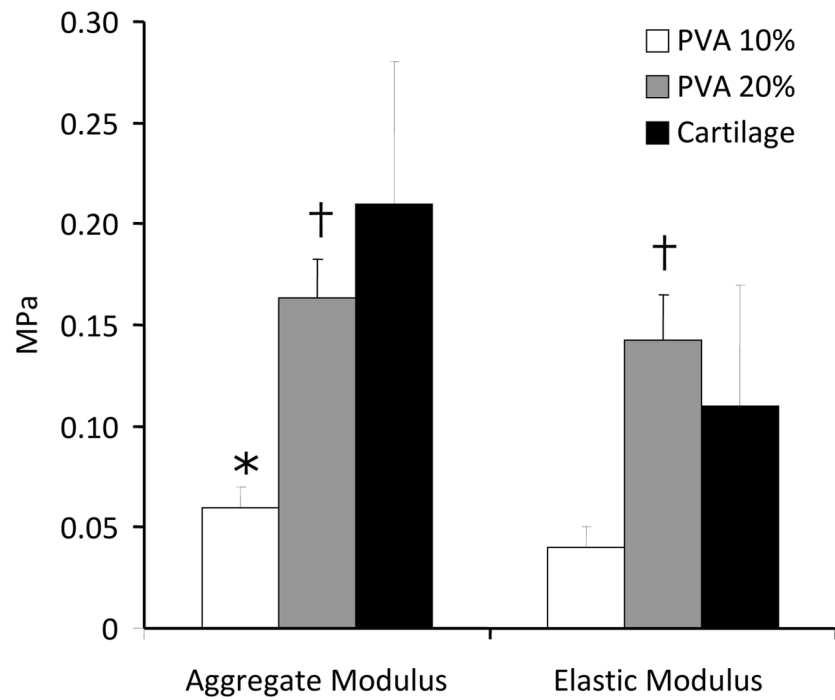
Figure 4.
Aggregate Modulus (H_A) and Elastic Modulus (E_S) of 10% PVA constructs and 20% PVA constructs vs. that of mature articular cartilage (n=6 samples per group). *p<0.05 vs. cartilage, †p<0.05 vs. 10% PVA
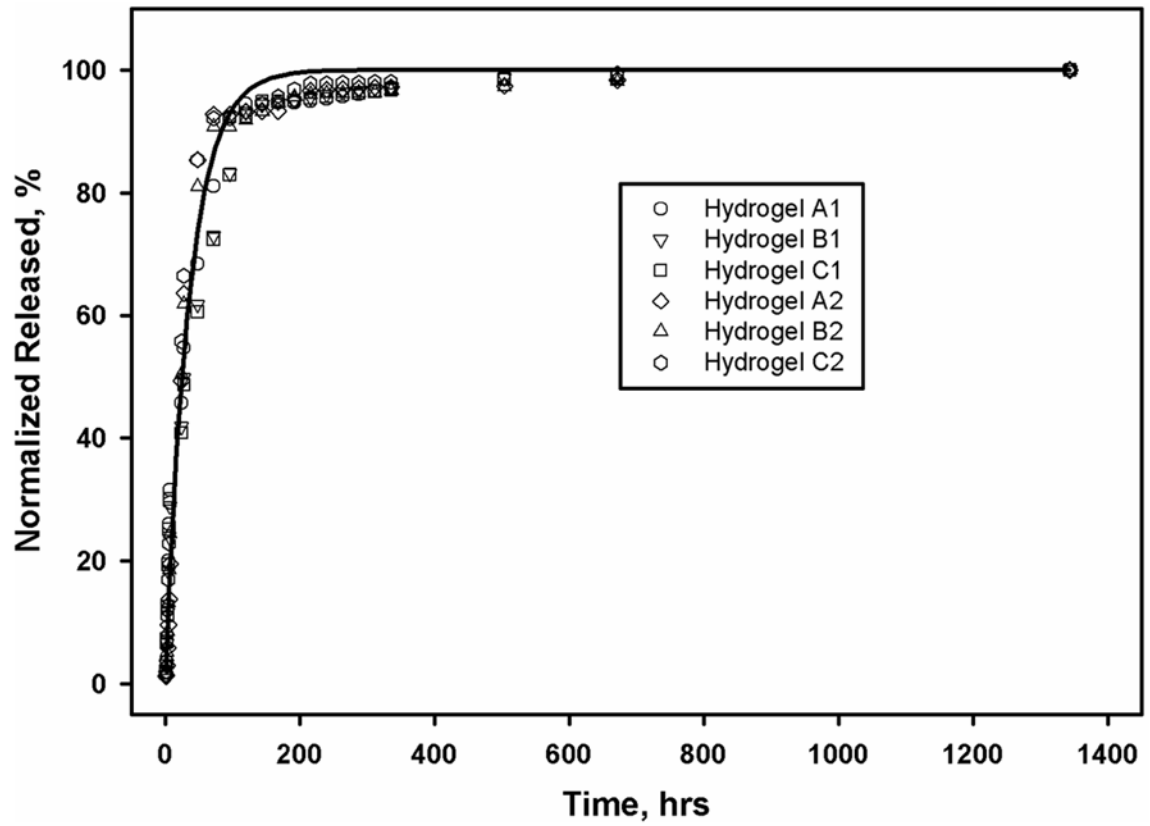
Figure 5.
The cumulative release of insulin from n=6 scaffolds up to 28 days. The release profile followed an exponential curve with a half-life of 25 hours.
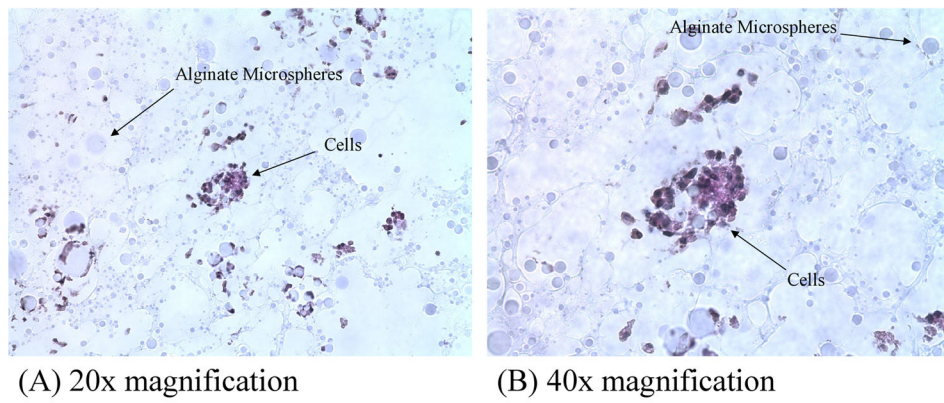
(A) 20x magnification   (B) 40x magnification

Figure 6.
Photomicrographs of Alcian Blue-stained cells present in the center of the PVA hydrogels at
(A) 20× magnification and (B) 40× magnification. After 14 days of seeding, cells were seen
to migrate inward from the injection sites.

Table 1

Cartilage and construct dynamic modulus (E_D) as a function of applied strain

Strain	Unconfined E_D (MPa)			Confined E_D (MPa)		
	Cartilage	10% PVA	20% PVA	Cartilage	10% PVA	20% PVA
4%	2.901 ± 1.668	0.068 ± 0.014[*]	0.159 ± 0.038[*†]	0.828 ± 0.607	0.134 ± 0.049[*]	0.593 ± 0.607[†]
8%	3.904 ± 2.364	0.084 ± 0.011[*]	0.165 ± 0.032[*†]	1.731 ± 1.018	0.340 ± 0.233[*]	1.843 ± 0.487[†]
12%	5.382 ± 2.868	0.088 ± 0.011[*]	0.191 ± 0.015[*†]	3.094 ± 1.351	0.412 ± 0.275[*]	4.372 ± 0.950[†]

[*] p<0.05 vs. cartilage,

[†] p<0.05 vs. 10% PVA

Table 2

Cartilage and construct permeability (k) as a function of % strain as determined from curve-fits of confined compression data

Strain	Permeability k (m^4/N-s)		
	Cartilage	10% PVA	20% PVA
4%	2.04E-15 ± 2.99E-15	1.41E-15 ± 6.45E-16	1.33E-15 ± 1.32E-15
8%	5.46E-16 ± 6.19E-16	5.48E-16 ± 2.57E-16	7.83E-16 ± 5.92E-16
12%	1.15E-16 ± 8.72E-17	1.12E-15 ± 7.61E-16	3.12E-16 ± 2.02E-16